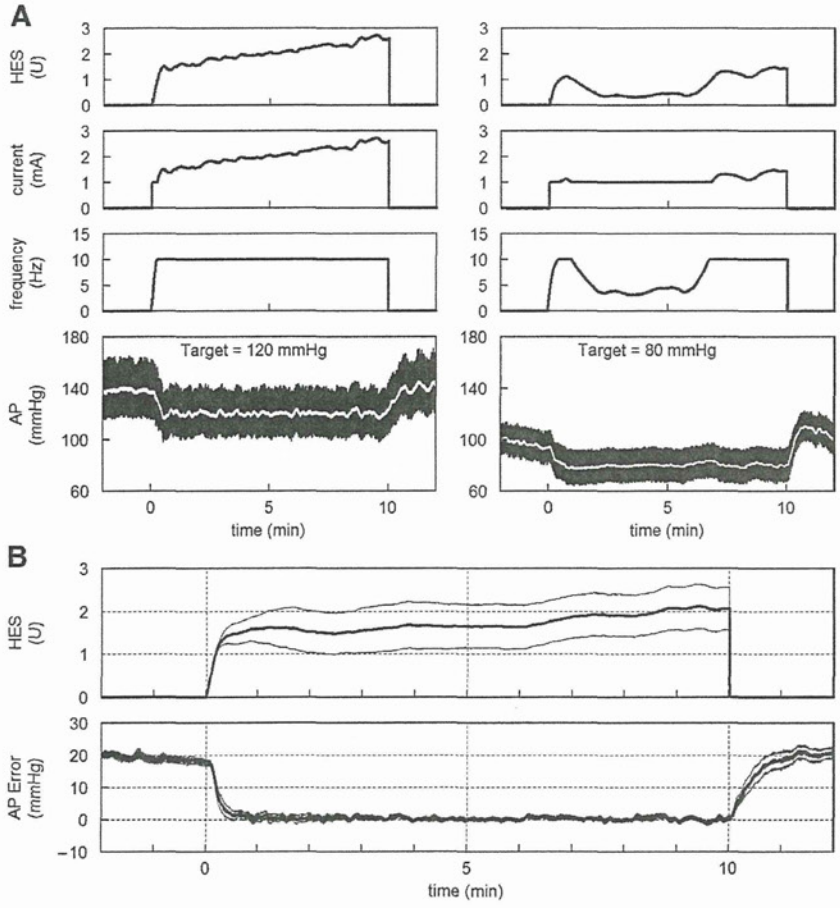

Figure 5. (**A**) Results of 10-min feedback control of arterial pressure (AP) by hind-limb electrical stimulation (HES) obtained from 2 cats. In each cat, the target AP was set at 20 mmHg below the baseline AP value. The current and frequency of HES were automatically adjusted to keep the AP at the target level. (**B**) HES command and the error signal between the target AP and measured AP averaged from 8 cats. The thick and thin lines indicate mean ± SE values, respectively.

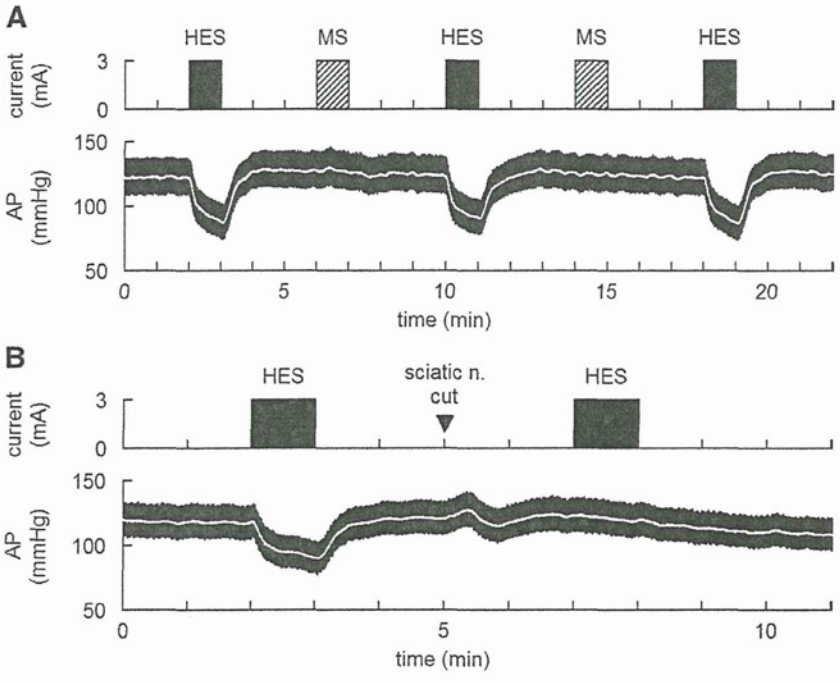

Figure 6. (**A**) Effects of electrical stimulation of the triceps surae muscle (MS) in comparison to hind-limb electrical stimulation (HES). Although muscle twitching was observed, there was no change in arterial pressure (AP) during MS. (**B**) Effects of sectioning the ipsilateral sciatic nerve on the HES-induced changes in AP. After the severance of the ipsilateral sciatic nerve, HES no longer produced significant hypotension.

from 1 to 7 min of the 10-min regulation. In this time period, the HES command altered the stimulus frequency rather than the stimulus current.

Mean and mean ± SE values of the HES command averaged from 8 animals are shown in the top panel of **Figure 5B**. There was a large variance in the HES command among the animals, suggesting inter-individual differences in the responsiveness to HES. The target AP was 102.5±5.6 mmHg across the animals. The error signal between the target AP and measured AP disappeared in less than 1 min (**Figure 5B**,

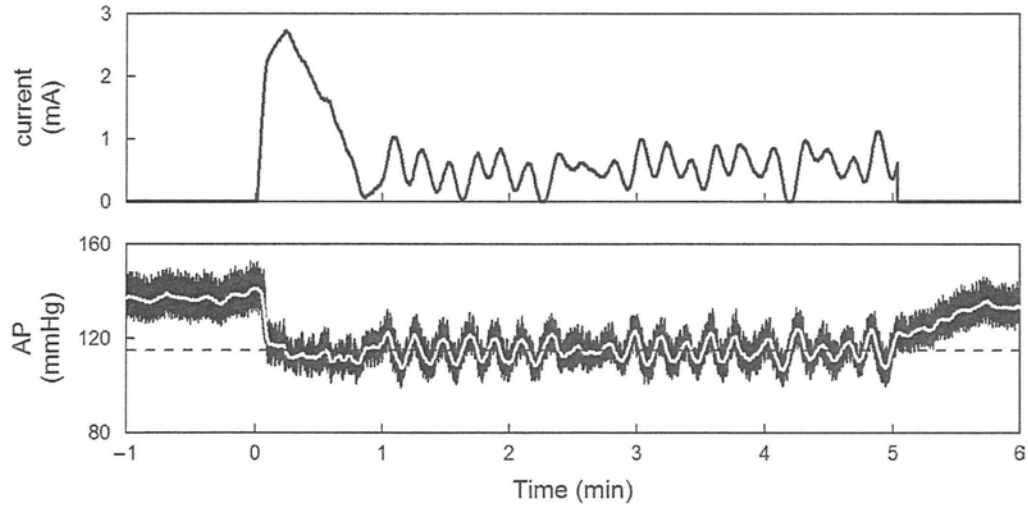

Figure 7. Typical recordings showing failure of controlling the intensity of the hind-limb electrical stimulation during the course of controller development. In this experimental run, only the stimulus current was controlled with a fixed stimulus frequency at 10 Hz. The controller showed on–off type controller behavior once the arterial pressure (AP) approached the target level. The horizontal dashed line indicates the target AP level.

Bottom). The time required for the AP response to reach 90% of the target AP decrease was 38±10 s. Thereafter, the error remained very small until the end of the 10-min regulation. The standard deviation of the steady-state error was 1.3±0.1 mmHg. After the end of the feedback regulation, the error signal gradually returned to approximately 20 mmHg.

Figure 6 represents typical results of the supplemental protocols. Electrical stimulation of the triceps surae muscle (denoted as "MS") did not change AP significantly in spite of visible twitching of the stimulated muscle, suggesting that the depressor response to HES was not the outcome of the direct muscle stimulation (**Figure 6A**). Sectioning the ipsilateral sciatic nerve abolished the depressor effect of HES, suggesting that somatic afferent signals were delivered through the sciatic nerve to the central nervous system during HES (**Figure 6B**).

Discussion

We identified the dynamic input–output relationship between HES and the AP response. By using the model transfer function from HES to AP, we were able to develop a servo-controller that automatically adjusted the HES command to reduce AP at a prescribed target level.

Development of the Feedback Controller

The stimulus current-AP response relationship showed a monotonous decreasing slope (**Figure 2C**). Because the effect of the pulse width was statistically insignificant, we chose the stimulus current as a primary control variable. The problem with using the stimulus current for the control variable was that a certain threshold current existed between 0 and 1 mA where the AP response to HES became discontinuous. If the stimulus current happened to be feedback controlled near the threshold current, AP showed significant oscillation around the target level (**Figure 7**, see Appendix B for details). To avoid such a problem related to the threshold current, we set the minimum current to 1 mA (above the threshold current) and used the stimulus frequency as a secondary control variable (**Figure 4B**).

The stimulus frequency-AP response relationship revealed a valley-shaped curve with the nadir of approximately 10 Hz (**Figure 2D**). The result is similar to that obtained by stimulating hamstring muscle afferent nerves.[26] From the viewpoint of controller design, the valley-shaped input–output relationship is troublesome because the proportional-integral controller only assumes a monotonous input–output relationship.[23] To avoid the problem of the valley-shaped input–output relationship, we limited the stimulus frequency to the range from 0 to 10 Hz (**Figure 4B**, **Right**). A similar strategy of selecting the monotonous input–output portion was used in a previous study.[12]

We quantified the dynamic AP response to HES using a transfer function analysis (**Figure 3B**), and modeled it by a second-order low-pass filter with a pure dead time (**Figure 3C**). Once the transfer function is modeled, we could construct a numerical simulator for the feedback controller design (**Figure 4A**). Because the optimization of control parameters usually requires a number of trials, even if the initial values are selected via classical methods such as the Ziegler–Nichols' method,[23] it is impractical to determine optimal parameter values without using the simulator. The simulation results indicated that the integral gain value of 0.005 would provide rapid and stable AP regulation (**Figure 4C**). Because the controller was designed via intensive simulations, AP was actually controlled at the target level with a small variance (**Figure 5B**, **Bottom**). Note that the current and frequency of HES were automatically adjusted and individualized via the feedback mechanism (**Figure 5A**).

Bionic Strategies Using Neural Interfaces

A framework of treating cardiovascular diseases using neural interfaces is intriguing because the autonomic nervous system exerts powerful influences on the circulatory system. In previous studies, we identified the dynamic characteristics of the arterial baroreflex system and used them to design an artificial vasomotor center. The artificial vasomotor center was able to control AP by stimulating the celiac ganglia in anesthetized rats[10,11] or the spinal cord in anesthetized cats.[12] The strength and rapidity of the neural effect on the cardiovascular system compared with that of the

humoral effect[27,28] make the neural interventions desirable for the rapid and stable restoration of AP against acute disturbances such as those induced by postural changes. Gotoh et al demonstrated that a direct neural interface to the rostral ventrolateral medulla also enabled rapid and stable restoration of AP during nitroprusside-induced hypotension in conscious rats?[29] The bionic system to control AP has also been applied in human subjects![13]

Although the aforementioned bionic systems aimed to maintain AP against acute hypotension by increasing sympathetic nerve activity,[10–13,29] sympathoinhibition might also be required for the treatment of cardiovascular diseases accompanying sympathetic overactivity. Baroreceptor activation is one of the potential sympathoinhibitory neural modulation?[8,9] In the present study we only demonstrated a framework of short-term AP control by HES. With a development of proper implanting electrodes, however, we might be able to control AP chronically using HES. Although carotid sinus baroreceptor stimulation has a potential to treat drug-resistant hypertension,[9] it could activate peripheral chemoreflex by stimulating carotid bodies. HES might circumvent such unintentional chemoreflex activation. Another clinical implication will be the treatment of chronic heart failure. Although the vagal effect of HES was not evaluated in the present study, acupuncture stimulation might facilitate cardiac vagal activity?[30] Because chronic intermittent vagal nerve stimulation increased the survival of chronic heart failure rats,[7] chronic intermittent HES might be used as an alternative method of direct vagal nerve stimulation for the treatment of chronic heart failure.

Study Limitations

First, we did not identify the mechanism of HES. Because sectioning of the ipsilateral sciatic nerve abolished the AP response to HES (**Figure 6B**), somatic afferent is involved in the effect of HES. In a series of studies, Chao et al and Li et al demonstrated that electroacupuncture activated group III and IV fibers in the median nerves and inhibited sympathetic outflow via activation of μ- and δ-opioid receptors in the rostral ventrolateral medulla?[31,32] Whether a similar mechanism underlies in the rapid-onset and short-lasting effect of HES awaits further studies.

Second, we used pentobarbital anesthesia. Although peripheral neurotransmissions of norepinephrine and acetylcholine can be assessed under the same anesthesia,[28,33] because pentobarbital can suppress many neurotransmitters in the central nervous system,[34] anesthesia might compromise the HES effect. Further studies are required to establish the utility of HES in awake conditions.

Third, we set the proportional gain of the controller at zero to avoid pulsatile changes in the HES command. However, other approaches such as that using a low-passed signal of measured AP as a controlled variable might also be effective to avoid the pulsatile variation in the HES command.

Finally, a development of implanting electrodes is the prerequisite for chronic use of HES. Intramuscular electrodes used in functional electrical stimulation might be used for HES but further refinements are clearly needed regarding the positioning of electrodes including the depth of implantation.[35,36]

In conclusion, we identified the dynamic characteristics of the AP response to acupuncture-like HES and demonstrated that a servo-controlled HES system was able to reduce AP at a prescribed target level. Although further studies are required to identify the mechanism of HES to reduce AP, acupuncture-like HES would be an additional modality to exert a quantitative depressor effect on the cardiovascular system.

Acknowledgments

This study was supported by the following Grants: "Health and Labour Sciences Research Grant for Research on Advanced Medical Technology", "Health and Labour Sciences Research Grant for Research on Medical Devices for Analyzing, Supporting and Substituting the Function of Human Body", "Health and Labour Sciences Research Grant (H18-Iryo-Ippan-023) (H18-Nano-Ippan-003) (H19-Nano-Ippan-009)", from the Ministry of Health, Labour and Welfare of Japan, and the "Industrial Technology Research Grant Program" from New Energy and Industrial Technology Development Organization of Japan.

References

1. Bilgutay AM, Bilgutay IM, Merkel FK, Lillehei CW. Vagal tuning: A new concept in the treatment of supraventricular arrhythmias, angina pectoris, and heart failure. *J Thorac Cardiovasc Surg* 1968; **56:** 71–82.
2. Braunwald E, Epstein SE, Glick G, Wechsler AS, Braunwald NS. Relief of angina pectoris by electrical stimulation of the carotid-sinus nerves. *N Engl J Med* 1967; **277:** 1278–1283.
3. Schwartz SI, Griffith LS, Neistadt A, Hagfors N. Chronic carotid sinus nerve stimulation in the treatment of essential hypertension. *Am J Surg* 1967; **114:** 5–15.
4. Vanoli E, De Ferrari GM, Stramba-Badiale M, Hull SS Jr, Foreman RD, Schwartz PJ. Vagal stimulation and prevention of sudden death in conscious dogs with a healed myocardial infarction. *Circ Res* 1991; **68:** 1471–1481.
5. Yang JL, Chen GY, Kuo CD. Comparison of effect of 5 recumbent positions on autonomic nervous modulation in patients with coronary artery disease. *Circ J* 2008; **72:** 902–908.
6. Baba R, Koketsu M, Nagashima M, Inasaka H, Yoshinaga M, Yokota M. Adolescent obesity adversely affects blood pressure and resting heart rate. *Circ J* 2007; **71:** 722–726.
7. Li M, Zheng C, Sato T, Kawada T, Sugimachi M, Sunagawa K. Vagal nerve stimulation markedly improves long-term survival after chronic heart failure in rats. *Circulation* 2004; **109:** 120–124.
8. Zucker IH, Hackley JF, Cornish KG, Hiser BA, Anderson NR, Kieval R, et al. Chronic baroreceptor activation enhances survival in dogs with pacing-induced heart failure. *Hypertension* 2007; **50:** 904–910.
9. Mohaupt MG, Schmidli J, Luft FC. Management of uncontrollable hypertension with a carotid sinus stimulation device. *Hypertension* 2007; **50:** 825–828.
10. Sato T, Kawada T, Shishido T, Sugimachi M, Alexander J Jr, Sunagawa K. Novel therapeutic strategy against central baroreflex failure: A bionic baroreflex system. *Circulation* 1999; **100:** 299–304.
11. Sato T, Kawada T, Sugimachi M, Sunagawa K. Bionic technology revitalizes native baroreflex function in rats with baroreflex failure. *Circulation* 2002; **106:** 730–734.
12. Yanagiya Y, Sato T, Kawada T, Inagaki M, Tatewaki T, Zheng C, et al. Bionic epidural stimulation restores arterial pressure regulation during orthostasis. *J Appl Physiol* 2004; **97:** 984–990.
13. Yamasaki F, Ushida T, Yokoyama T, Ando M, Yamashita K, Sato T. Artificial baroreflex: Clinical application of a bionic baroreflex system. *Circulation* 2006; **113:** 634–639.
14. Li P, Pitsillides KF, Rendig SV, Pan HL, Longhurst JC. Reversal of reflex-induced myocardial ischemia by median nerve stimulation: A feline model of electroacupuncture. *Circulation* 1998; **97:** 1186–1194.
15. Longhurst JC. Electroacupuncture treatment of arrhythmias in myocardial ischemia. *Am J Physiol Heart Circ Physiol* 2007; **292:** H2032–H2034.
16. Lujan HL, Kramer VJ, DiCarlo SE. Electroacupuncture decreases the susceptibility to ventricular tachycardia in conscious rats by reducing cardiac metabolic demand. *Am J Physiol Heart Circ Physiol* 2007; **292:** H2550–H2555.
17. Ohsawa H, Okada K, Nishijo K, Sato Y. Neural mechanism of depressor responses of arterial pressure elicited by acupuncture-like stimulation to a hindlimb in anesthetized rats. *J Auton Nerv Syst* 1995; **51:** 27–35.
18. Uchida S, Shimura M, Ohsawa H, Suzuki A. Neural mechanism of bradycardiac responses elicited by acupuncture-like stimulation to a hind limb in anesthetized rats. *J Physiol Sci* 2007; **57:** 377–382.
19. Michikami D, Kamiya A, Kawada T, Inagaki M, Shishido T, Yamamoto K, et al. Short-term electroacupuncture at Zusanli resets the arterial baroreflex neural arc toward lower sympathetic nerve

activity. *Am J Physiol Heart Circ Physiol* 2006; **291:** H318–H326.
20. Yamamoto H, Kawada T, Kamiya A, Kita T, Sugimachi M. Electroacupuncture changes the relationship between cardiac and renal sympathetic nerve activities in anesthetized cats. *Auton Neurosci: Basic and Clinical* 2008; **144:** 43–49.
21. Marmarelis PZ, Marmarelis VZ. Analysis of Physiological Systems. The white noise method in system identification. New York: Plenum; 1978.
22. Snedecor GW, Cochran WG. Statistical Methods, 8th ed. Ames, Iowa: University Press; 1989.
23. Åström K, Hägglund T. PID Controllers: Theory, Design, and Tuning, 2nd ed. City of Publication: Instrument Society of America; 1995.
24. Kawada T, Sunagawa G, Takaki H, Shishido T, Miyano H, Miyashita H, et al. Development of a servo-controller of heart rate using a treadmill. *Jpn Circ J* 1999; **63:** 945–950.
25. Kawada T, Ikeda Y, Takaki H, Sugimachi M, Kawaguchi O, Shishido T, et al. Development of a servo-controller of heart rate using a cycle ergometer. *Heart Vessels* 1999; **14:** 177–184.
26. Johansson B. Circulatory responses to stimulation of somatic afferents with special reference to depressor effects from muscle nerves. *Acta Physiol Scand* 1962; **Suppl 198:** 1–91.
27. Kawada T, Miyamoto T, Miyoshi Y, Yamaguchi S, Tanabe Y, Kamiya A, et al. Sympathetic neural regulation of heart rate is robust against high plasma catecholamines. *J Physiol Sci* 2006; **56:** 235–245.
28. Kawada T, Yamazaki T, Akiyama T, Shishido T, Miyano H, Sato T, et al. Interstitial norepinephrine level by cardiac microdialysis correlates with ventricular contractility. *Am J Physiol Heart Circ Physiol* 1997; **273:** H1107–H1112.
29. Gotoh TM, Tanaka K, Morita H. Controlling arterial blood pressure using a computer-brain interface. *Neuroreport* 2005; **16:** 343–347.
30. Nishijo K, Mori H, Yosikawa K, Yazawa K. Decreased heart rate by acupuncture stimulation in humans via facilitation of cardiac vagal activity and suppression of cardiac sympathetic nerve. *Neurosci Lett* 1997; **227:** 165–168.
31. Chao DM, Shen LL, Tjen-A-Looi S, Pitsillides KF, Li P, Longhurst JC. Naloxone reverses inhibitory effect of electroacupuncture on sympathetic cardiovascular reflex responses. *Am J Physiol Heart Circ Physiol* 1999; **276:** H2127–H2134.
32. Li P, Tjen-A-Looi SC, Longhurst JC. Rostral ventrolateral medullary opioid receptor subtypes in the inhibitory effect of electroacupuncture on reflex autonomic response in cats. *Auton Neurosci: Basic and Clinical* 2001; **89:** 38–47.
33. Kawada T, Yamazaki T, Akiyama T, Li M, Ariumi H, Mori H, et al. Vagal stimulation suppresses ischemia-induced myocardial interstitial norepinephrine release. *Life Sci* 2006; **78:** 882–887.
34. Adachi YU, Yamada S, Satomoto M, Watanabe K, Higuchi H, Kazama T. et al. Pentobarbital inhibits L-DOPA-induced dopamine increases in the rat striatum: An in vivo microdialysis study. *Brain Res Bull* 2006; **69:** 593–596.
35. Guevremont L, Norton JA, Mushahwar VK. Physiologically based controller for generating overground locomotion using functional electrical stimulation. *J Neurophysiol* 2007; **97:** 2499–2510.
36. Hardin E, Kobetic R, Murray L, Corado-Ahmed M, Pinault G, Sakai J, et al. Walking after incomplete spinal cord injury using an implanted FES system: A case report. *J Rehabil Res Dev* 2007; **44:** 333–346.

Appendix A

Framework of the Feedback Controller

Figure 4A is a simplified block diagram of the feedback controller system used in the present study. The controller was based on a proportional-integral controller[23–25] $G(f)$ represents the transfer function of the controller.

$$G(f)=-K_P+\frac{-K_I}{2\pi fj} \quad \text{(A1)}$$

where K_P and K_I denote proportional and integral gains, respectively. j represents the imaginary unit. Negative signs for the proportional and integral gains compensate for the negative input–output relationship between HES and the AP response. $H(f)$ represents a model transfer function from HES to AP determined from Protocol 3. The measured AP can be expressed as:

$$AP_{Measured}(f)=H(f)HES(f)+AP_{Noise}(f) \quad \text{(A2)}$$

where $AP_{Noise}(f)$ is the AP fluctuation such as that associated with changes in animal conditions. The controller compares the measured AP with the target AP, and adjusts the HES command to minimize the difference between them according to the following equation:

$$HES(f)=G(f)[AP_{Target}(f)-AP_{Measured}(f)] \quad \text{(A3)}$$

By eliminating $HES(f)$ from the equations A2 and A3, the overall controller characteristics are described as:

$$AP_{Measured}(f)=\frac{G(f)H(f)}{1+G(f)H(f)}AP_{Target}(f)+\frac{1}{1+G(f)H(f)}AP_{Noise}(f) \quad \text{(A4)}$$

The equation A4 indicates that if $G(f)$ is properly selected so that $G(f)H(f)$ becomes by far greater than unity, the measured AP approaches the target AP whereas the noise term is significantly attenuated over the frequency range of interest.

Appendix B

Problem with the Threshold Current

We tried to adjust the intensity of HES by the stimulus current alone. When the stimulus current happened to be feedback controlled near a threshold current, however, the controller showed an on–off type controller behavior around the target AP level, as shown in **Figure 7**. At time zero, the controller was activated. The stimulus current increased to approximately 2.7 mA in the beginning and then decreased to a value below 1 mA, accompanying the AP reduction around a target level (a horizontal dashed line). However, the stimulus current and AP did not stabilize. Because the AP response was discontinuous at the threshold current (ie, the depressor effect of HES was abruptly turned on and off), the controller could not adjust the stimulus current in a continuous manner. To avoid this kind of on–off type controller behavior, we introduced the stimulus frequency as the secondary control variable (**Figure 4B**).

Inhibition of Tumor Necrosis Factor-α–Induced Interleukin-6 Expression by Telmisartan Through Cross-Talk of Peroxisome Proliferator-Activated Receptor-γ With Nuclear Factor κB and CCAAT/Enhancer-Binding Protein-β

Qingping Tian, Ryohei Miyazaki, Toshihiro Ichiki, Ikuyo Imayama, Keita Inanaga, Hideki Ohtsubo, Kotaro Yano, Kotaro Takeda, Kenji Sunagawa

Abstract—Telmisartan, an angiotensin II type 1 receptor antagonist, was reported to be a partial agonist of peroxisome proliferator-activated receptor-γ. Although peroxisome proliferator-activated receptor-γ activators have been shown to have an anti-inflammatory effect, such as inhibition of cytokine production, it has not been determined whether telmisartan has such effects. We examined whether telmisartan inhibits expression of interleukin-6 (IL-6), a proinflammatory cytokine, in vascular smooth muscle cells. Telmisartan, but not valsartan, attenuated IL-6 mRNA expression induced by tumor necrosis factor-α (TNF-α). Telmisartan decreased TNF-α–induced IL-6 mRNA and protein expression in a dose-dependent manner. Because suppression of IL-6 mRNA expression was prevented by pretreatment with GW9662, a specific peroxisome proliferator-activated receptor-γ antagonist, peroxisome proliferator-activated receptor-γ may be involved in the process. Telmisartan suppressed IL-6 gene promoter activity induced by TNF-α. Deletion analysis suggested that the DNA segment between −150 bp and −27 bp of the IL-6 gene promoter that contains nuclear factor κB and CCAAT/enhancer-binding protein-β sites was responsible for telmisartan suppression. Telmisartan attenuated TNF-α–induced nuclear factor κB– and CCAAT/enhancer-binding protein-β–dependent gene transcription and DNA binding. Telmisartan also attenuated serum IL-6 level in TNF-α–infused mice and IL-6 production from rat aorta stimulated with TNF-α ex vivo. These data suggest that telmisartan may attenuate inflammatory process induced by TNF-α in addition to the blockade of angiotensin II type 1 receptor. Because both TNF-α and angiotensin II play important roles in atherogenesis through enhancement of vascular inflammation, telmisartan may be beneficial for treatment of not only hypertension but also vascular inflammatory change. (***Hypertension*. 2009;53: 798-804.**)

Key Words: interleukin-6 ■ TNF-α ■ PPARγ ■ NF-κB ■ C/EBPβ

Angiotensin II (Ang II) is a main final effecter molecule of the renin–angiotensin system. Physiologically, Ang II plays an important role in the regulation of blood pressure, fluid volume, and electrolyte balance.[1] However, Ang II is also involved in the pathological processes, such as cardiovascular diseases, renal insufficiency, and metabolic disorders.[2] Indeed, inhibition of the renin–angiotensin system by Ang II type 1 receptor (AT1R) antagonists has been proven beneficial for treatment of heart failure,[3] chronic kidney diseases,[4] and myocardial infarction.[5] AT1R antagonists also showed favorable effects on prevention of new onset of diabetes mellitus and atrial fibrillation.[6,7]

Telmisartan, one of the AT1R antagonists, was reported to be a partial agonist of peroxisome proliferator-activated receptor-γ (PPARγ).[8,9] PPARγ is a nuclear receptor transcription factor,[10] and the target genes of PPARγ are involved in the regulation of lipid and glucose metabolism and adipocyte differentiation. In addition, it is reported that thiazolidinediones (TZDs), synthetic PPARγ ligands, have an anti-inflammatory effect and inhibit atherogenesis.[11] The anti-inflammatory effect of TZDs involves inhibition of the function of nuclear factor κB (NF-κB), which plays an important role in the expression of many genes mediating an inflammatory process.[12]

Interleukin-6 (IL-6) is one of the proinflammatory cytokines and is induced by tumor necrosis factor-α (TNF-α),[13] Ang II,[14] and other stimuli in vascular smooth muscle cells (VSMCs), endothelial cells, and macrophages. IL-6 plays an

Received November 17, 2008; first decision November 24, 2008; revision accepted February 23, 2009.

From the Departments of Cardiovascular Medicine (Q.T., R.M., T.I., I.I., K.I., H.O., K.Y., K.T., K.S.) and Advanced Therapeutics for Cardiovascular Diseases (T.I., K.T.), Kyushu University Graduate School of Medical Sciences, and Peking University First Hospital (Q.T.), Fukuoka, Japan.

Q.T., R.M., and I.I. contributed equally to this work.

Correspondence to Toshihiro Ichiki, MD, PhD, Department of Cardiovascular Medicine, Kyushu University Graduate School of Medical Sciences, 3-1-1 Maidashi, Higashi-ku, 812-8582 Fukuoka, Japan. E-mail ichiki@cardiol.med.kyushu-u.ac.jp

Hypertension **is available at http://hyper.ahajournals.org** **DOI: 10.1161/HYPERTENSIONAHA.108.126656**

important role in vascular remodeling and was reported to be a useful biomarker in predicting future cardiovascular events.[15]

Telmisartan has been shown to induce differentiation of adipocytes through activation of PPARγ. A recent study showed that telmisartan attenuated hepatic steatosis, inflammation, and fibrosis in a rat model of nonalcoholic steatohepatitis.[16] It was also reported that telmisartan treatment of patients with hypertension and coronary heart disease decreased β2-integrin MAC-1 expression in peripheral lymphocytes independent of Ang II.[17] These data suggest that telmisartan has an anti-inflammatory effect independently of AT1R blocking effect. However, an anti-inflammatory effect of telmisartan on blood vessel is incompletely characterized. Therefore, we tested whether telmisartan inhibits TNF-α–induced IL-6 expression through PPARγ in VSMCs.

Materials and Methods

DMEM was purchased from GIBCO/BRL. FBS was from JRH Biosciences. Recombinant TNF-α was a generous gift from Dainippon-Sumitomo Pharmaceutical Co (Osaka, Japan). Telmisartan was a generous gift from Boehringer Ingelheim (Ingelheim, Germany). Valsartan was purchased from US Pharmacopeia. BSA and GW9662 were purchased from Sigma. Pioglitazone was purchased from LKT Laboratories. [α-^{32}P] dCTP and [γ-^{32}P]ATP were purchased from Perkin-Elmer Life Sciences. Antibodies against extracellular signal-regulated protein kinase (ERK), p38 mitogen-activated protein kinase (MAPK), c-Jun N-terminal kinase (JNK), and their phosphorylated forms were purchased from Cell Signaling Technology. Other reagents were purchased from Wako Pure Chemicals unless otherwise mentioned specifically. TNF-α was dissolved in DMEM with 0.1% BSA, and Ang II was suspended in sterile water. Other reagents that added to culture medium were dissolved in dimethyl sulfoxide at a final concentration of 0.1%, which did not show any effect on IL-6 induction.

Cell Culture

VSMCs were isolated from the thoracic aorta of Sprague–Dawley rats and cultured in a humidified atmosphere of 95% air/5% CO_2 at 37°C in DMEM as described previously.[14] Cells were grown to confluence and growth-arrested in DMEM with 0.1% BSA for 2 days before use. Passages between 5 and 13 were used for the experiments.

Northern Blotting

Total RNA was prepared according to the acid guanidinium thiocyanate-phenol-chloroform extraction method. Northern blot analysis of IL-6 mRNA and 18S ribosomal RNA (rRNA) was performed as described previously.[14] The radioactivity of hybridized bands of IL-6 mRNA and rRNA was quantified with a MacBAS Bioimage Analyzer (Fuji Photo Film). It was reported that 2 species of IL-6 mRNA were generated by an alternative polyadenylation.[18] The intensity of both bands was taken into account for quantification.

Quantification of Rat IL-6 by Sandwich ELISA

VSMCs were stimulated with TNF-α (10 ng/mL) or Ang II (100 nmol/L) for 24 hours in the presence or absence of telmisartan (1 to 20 μmol/L). Then the medium of VSMCs was collected and centrifuged at 12 000 rpm for 1 minute. The supernatant was stored at −70°C until used for the assay. ELISA for rat IL-6 was performed with a Cytoscreen ELISA kit (BioSource International) according to manufacturer instructions. The measurement was performed in duplicate.

Transfection of IL-6 Promoter–Luciferase Fusion DNA Construct to VSMCs

The IL-6 gene promoter–luciferase fusion DNA constructs and luciferase assay were described previously.[14] Detailed protocols can be found in an online data supplement available at http://hyper.ahajournals.org.

Plasmids of NF-κB–luciferase and CCAAT/enhancer-binding protein-β (C/EBPβ)–luciferase were purchased from Stratagene Co. Five copies of NF-κB consensus sequence or 3 copies of C/EBPβ consensus sequence were ligated to minimal promoter followed by luciferase gene.

Gel Mobility Shift Assay

Gel mobility shift assay was performed as described previously[14] using synthetic NF-κB and C/EBPβ DNA probe (NF-κB: CAT GTG GGA TTT TCC CAT GA; C/EBPβ: CAC ATT GCA CAA TCT TAA). Detailed protocols are indicated in the online supplement.

Effect of Telmisartan on Ang II– and TNF-α–Induced IL-6 Production In Vivo

All procedures were approved by the institutional animal use and care committee and were conducted in conformity with institutional guidelines of Kyushu University. Ang II (490 ng/kg per minute) or TNF-α (80 ng/kg per minute) was administered subcutaneously to 9-week-old C57/BL6 mice (Kyudo Co; Saga, Japan) by osmotic mini-pump (Alzet) for 1 week. Doses of TNF-α and Ang II were determined in a preliminary experiment to detect a significant increase in the serum IL-6 level. Telmisartan was dissolved in water (10 μg/mL) and administered ad libitum. The estimated dose of orally ingested telmisartan was 2 mg/kg per day. Blood pressure and heart rate were measured using tail-cuff method (UR-5000; UEDA). After 1 week, mice were euthanized under pentobarbital anesthesia, and peripheral blood was collected from inferior vena cava. The serum concentration of IL-6 was measured using ELISA kit (R&D Systems). No significant differences in body weight were observed among the treatment groups (data not shown).

Ex Vivo Stimulation of Rat Aorta

Nine-week-old Sprague-Dawley rats were purchased from Kyudo Co. Rats were euthanized under deep pentobarbital anesthesia. The aorta was excised and adventitia was removed. The aorta was cut into 6 pieces and stimulated with TNF-α (50 ng/mL) or Ang II (1 μmol/L) in the absence or presence of telmisartan (10 μmol/L) in 500 μL of DMEM supplemented with 0.1% BSA for 48 hours. Concentrations of Ang II and TNF-α were determined in a preliminary experiment to detect a significant increase in the production of IL-6 in the supernatant of ex vivo–cultured aortic segments. The supernatant was subjected to ELISA to measure IL-6 production. The IL-6 concentration in the supernatant was normalized with the wet weight of the aortic segment.

RT-PCR and Western Blot Analysis

Detailed protocols are indicated in the online supplement.

Statistical Analysis

Statistical analysis was performed with 1-way ANOVA and Fisher's test if appropriate. A P value <0.05 was considered statistically significant. Values are expressed as mean±SEM.

Results

Telmisartan Attenuated TNF-α–Induced IL-6 Expression

VSMCs were incubated with or without telmisartan (10 μmol/L) for 60 minutes. Then the cells were stimulated with TNF-α (10 ng/mL) for 30 minutes. Northern blot analysis revealed attenuation of TNF-α–induced IL-6 mRNA expression by telmisartan (Figure 1A). However, valsartan (10 μmol/L), another AT1R antagonist, failed to suppress TNF-α–induced IL-6 mRNA expression (Figure 1B). Telmisartan (1 to 20 μmol/L) dose-dependently suppressed TNF-α–induced IL-6 mRNA expression (Figure 1C). The concentration range of telmisartan was chosen based on a previous

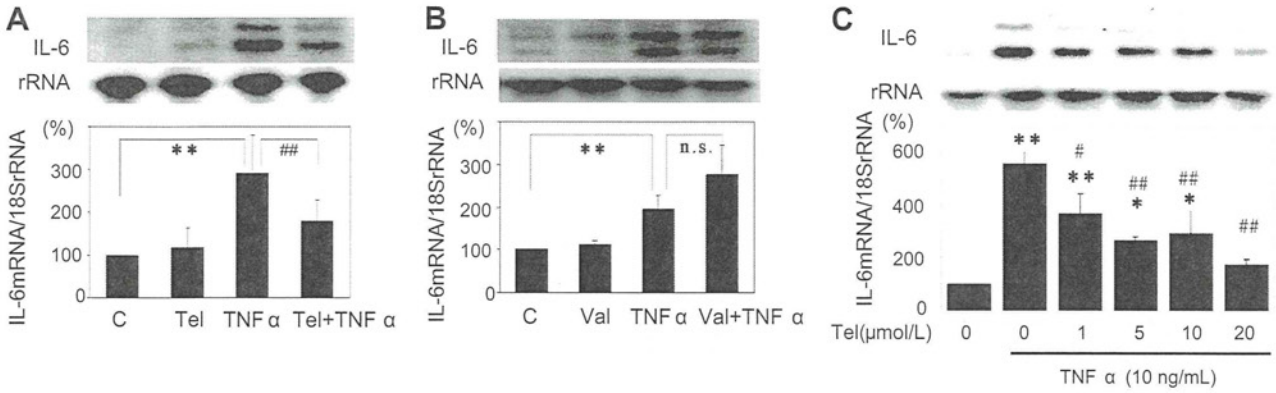

Figure 1. Suppression of TNF-α–induced IL-6 mRNA expression by telmisartan (Tel). VSMCs were preincubated with Tel (10 μmol/L; A), valsartan (Val; 10 μmol/L; B), or various concentrations (1 to 20 μmol/L; C) of telmisartan for 60 minutes and stimulated with TNF-α (10 ng/mL) for 30 minutes. Total RNA was isolated, and expression of IL-6 mRNA and 18S rRNA was determined by Northern blot analysis. Radioactivity of IL-6 mRNA was measured with an imaging analyzer and was normalized by radioactivity of rRNA. Values (mean±SEM) are expressed as percentage of control culture in a bar graph (100%; No. of independent experiments was 5). *P<0.05; **P<0.01 vs control; #P<0.05; ##P<0.01 vs TNF-α.

clinical study[19] that showed that the steady-state serum level of telmisartan was 1 to 5 μmol/L when 80 to 160 mg per day of telmisartan was given for 7 days to patients with essential hypertension. And it was reported that telmisartan at concentrations >25 μmol/L stimulated PPARα.[9] Therefore, we did not use telmisartan at concentrations >20 μmol/L in this study.

The protein level of IL-6 in the supernatant of VSMCs was measured after 24 hours of stimulation with TNF-α (10 ng/mL) with or without preincubation with telmisartan (1 to 20 μmol/L). TNF-α–induced IL-6 protein expression was also dose-dependently attenuated by telmisartan (Figure 2A). Ang II (100 nmol/L)–induced IL-6 production was inhibited completely by telmisartan at lower concentrations (Figure 2B); thus, we confirmed that telmisartan is an effective AT1R antagonist.

We next examined whether telmisartan affected TNF receptor expression. Semiquantitative RT-PCR analysis showed that telmisartan did not affect TNF type 1 receptor mRNA expression (supplemental Figure IB). We could not detect TNF type 2 receptor mRNA in our VSMCs. We also examined the effect of telmisartan on TNF-α–induced MAPK activation (supplemental Figure II). Telmisartan did not affect TNF-α–induced activation of ERK, p38MAPK, or JNK.

Telmisartan Inhibition of TNF-α–Induced IL-6 Expression Was Dependent on PPARγ

To clarify the role of PPARγ in telmisartan inhibition of TNF-α–induced IL-6 expression, the effect of GW9662, a PPARγ-specific antagonist, was examined. Although GW9662 itself did not affect IL-6 mRNA expression, preincubation with GW9662 (10 μmol/L; 3 hours) blocked telmisartan inhibition of TNF-α–induced IL-6 expression (Figure 3A). Pioglitazone (10 μmol/L; preincubation for 1 hour), a full PPARγ agonist, also suppressed the TNF-α–induced IL-6 mRNA expression (Figure 3B).

Telmisartan-Inhibited IL-6 Gene Promoter Activity

Next, the effect of telmisartan on IL-6 gene promoter activity was examined. TNF-α (10 ng/mL) increased IL-6 gene promoter activity by 2-fold. Preincubation with telmisartan (10 μmol/L) significantly inhibited IL-6 gene promoter activity (Figure 4). Deletion analysis of the IL-6 gene promoter suggested that the DNA segment between −150 bp and −27 bp was responsible for the downregulation by telmisartan (Figure 4A) because telmisartan inhibited the luciferase activity in the −150-bp construct, but the −27-bp

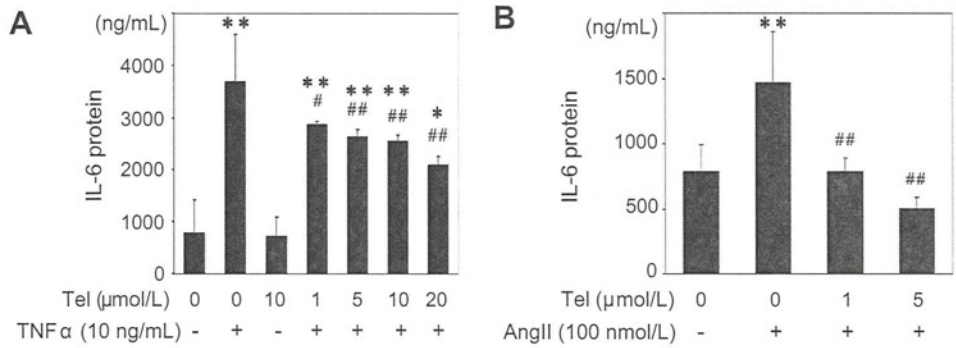

Figure 2. Suppression of TNF-α– and Ang II–induced IL-6 protein production by telmisartan (Tel). A, VSMCs were preincubated with Tel (10 μmol/L) at various concentrations for 60 minutes and stimulated with TNF-α (10 ng/mL) for 24 hours. B, VSMCs were incubated with Tel at 1 or 5 μmol/L and stimulated with Ang II (100 nmol/L) for 24 hours. IL-6 protein production in the supernatant of VSMCs was measured by ELISA. *P<0.05 vs control; **P<0.01 vs control; #P<0.05 vs TNF-α; ##P<0.01 vs TNF-α or Ang II (No. of independent experiment was 6 in duplicate).

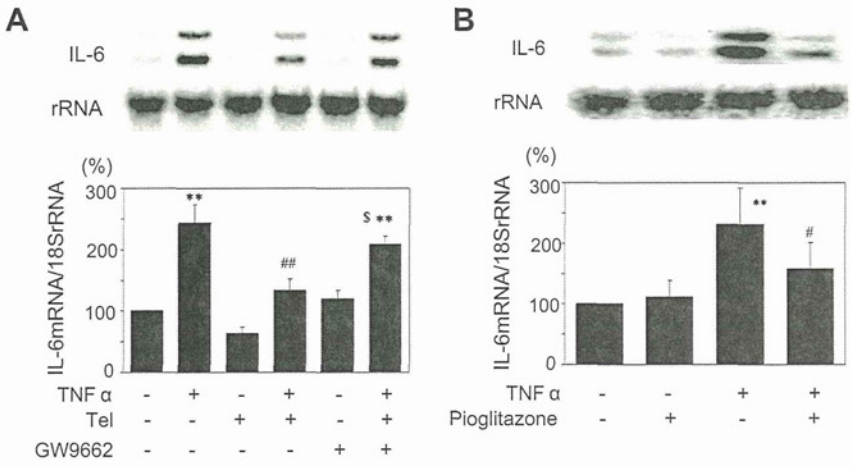

Figure 3. Effect of GW9662 on telmisartan (Tel) inhibition of TNF-α–induced IL-6 expression. A, VSMCs were incubated with GW9662 (10 μmol/L) for 3 hours followed by preincubation with Tel (10 μmol/L) for 60 minutes. Then the VSMCs were stimulated with TNF-α (10 ng/mL) for 30 minutes. B, VSMCs were preincubated with pioglitazone (10 μmol/L) for 60 minutes, then stimulated with TNF-α (10 ng/mL) for 30 minutes. Northern blot analysis of IL-6 mRNA was performed as described in Figure 1 legend. $^{**}P<0.01$ vs control; #$P<0.05$ vs TNF-α; ## $P<0.01$ vs TNF-α; \$$P<0.05$ vs Tel+TNF-α (No. of independent experiments was 4).

construct no longer responded to TNF-α or telmisartan. The DNA segment between −150 bp and −27 bp contains NF-κB and C/EBPβ as consensus cis DNA elements.[20] We therefore examined whether telmisartan inhibited NF-κB– and C/EBPβ-dependent gene transcription activated by TNF-α. As shown in Figure 4B, telmisartan inhibited TNF-α–induced activation of luciferase activity, which is solely dependent on NF-κB or C/EBPβ.

The gel mobility shift assay showed that telmisartan inhibited TNF-α–induced NF-κB DNA binding activity (Figure 5A). Telmisartan also attenuated TNF-α–induced C/EBPβ DNA binding activity to a lesser extent (Figure 5B).

Telmisartan Attenuated IL-6 Production In Vivo and Ex Vivo

To confirm that telmisartan inhibits IL-6 production in vivo, Ang II (490 ng/kg per minute) or TNF-α (80 ng/kg per minute) was administered to mice with or without telmisartan (2 mg/kg per day) for 1 week. Ang II but not TNF-α increased blood pressure level (Table). Ang II–induced high blood pressure was inhibited by telmisartan. Heart rate was not significantly different among the treatment groups. Ang II–induced increase in serum IL-6 level was almost completely inhibited by telmisartan, and telmisartan significantly attenuated TNF-α–induced IL-6 production (Figure 6A). To

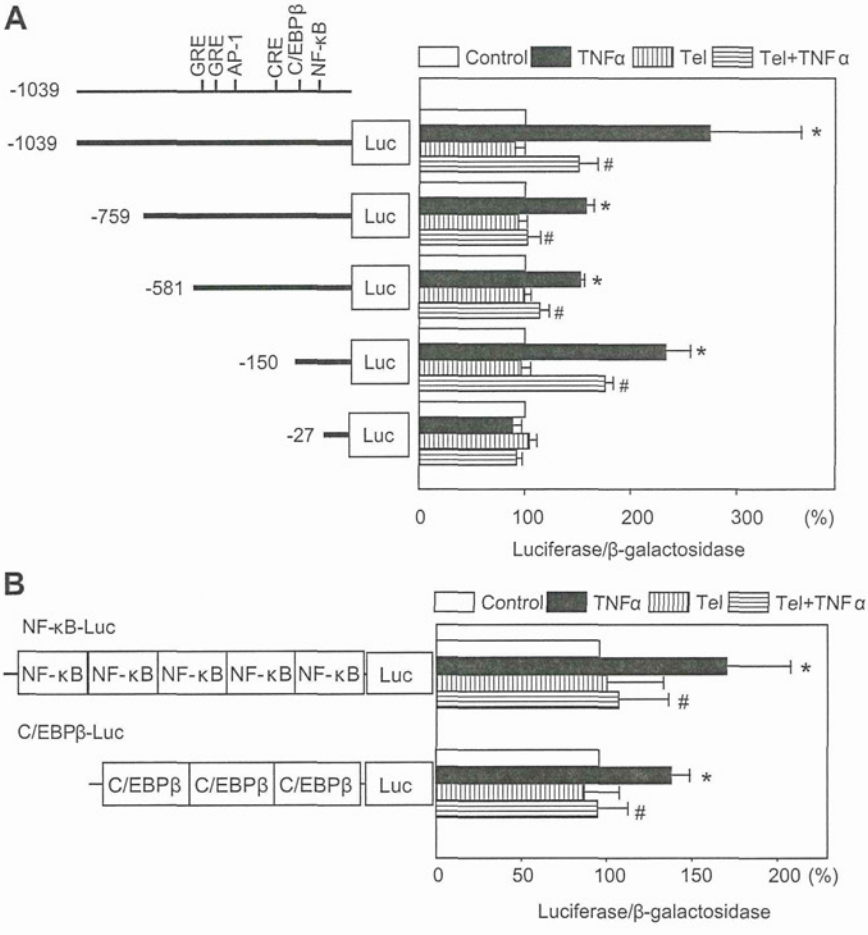

Figure 4. Suppression of IL-6 gene promoter activity by telmisartan (Tel). A, After transfection of IL-6 gene promoter/luciferase (Luc) fusion DNA (5 μg), VSMCs were preincubated with or without Tel (10 μmol/L; 60 minutes) and stimulated with TNF-α (10 ng/mL) for 24 hours. AP-1 indicates activator protein-1. B, NF-κB–Luc or C/EBPβ–Luc was introduced to VSMCs. VSMCs were preincubated with or without Tel (10 μmol/L; 60 minutes) and stimulated with TNF-α (10 ng/mL) for 24 hours. Luc activity was normalized with β-galactosidase activity. The relative promoter activity without stimulation (control) was set as 100%. *$P<0.01$ vs control; #$P<0.05$ vs TNF-α (No. of independent experiments was 4).

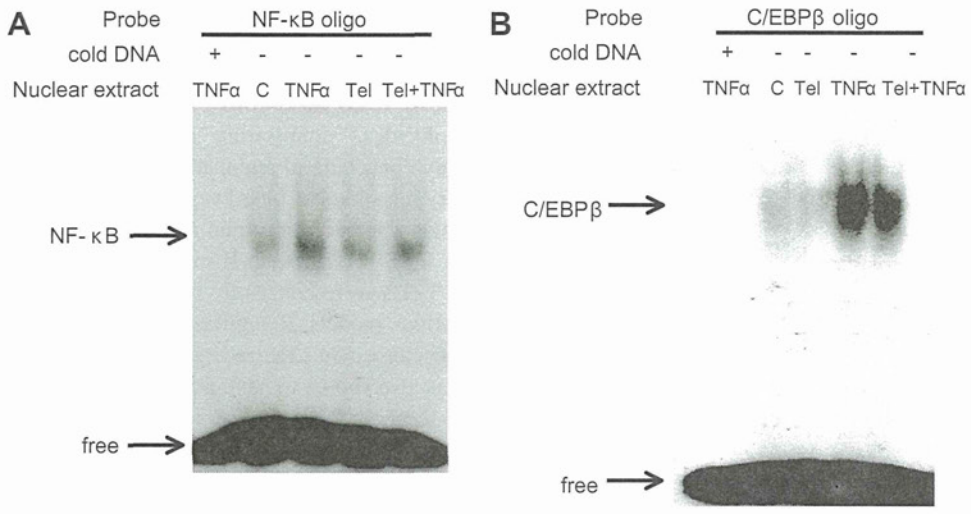

Figure 5. Telmisartan (Tel) attenuated TNF-α–induced NF-κB and C/EBPβ binding. A, Binding activity of NF-κB sequence of IL-6 gene promoter to nuclear extracts from unstimulated (C), TNF-α–stimulated, Tel-stimulated, and Tel- and TNF-α–stimulated VSMCs were examined by gel mobility shift assay. B, Binding activity of C/EBPβ sequence of IL-6 gene promoter to nuclear extracts from unstimulated, Tel-stimulated, TNF-α–stimulated, and Tel- and TNF-α–stimulated VSMCs were examined by gel mobility shift assay. Fifty times molar excess of unlabeled oligonucleotide (oligo) was added to the reaction mixture in the left lane (Cold DNA+). The same results were obtained in other independent experiments (No. of independent experiment was 3).

confirm that IL-6 is produced from blood vessel, a segment of rat aorta without adventitia was stimulated ex vivo with Ang II (1 μmol/L) or TNF-α (50 ng/mL) in the presence or absence of telmisartan (10 μmol/L) for 48 hours. Production of IL-6 induced by TNF-α in the supernatant was significantly attenuated by coincubation with telmisartan (Figure 6B). Ang II–induced production of IL-6 was completely inhibited by telmisartan. These results were consistent with those obtained during in vitro experiments.

Discussion

In the present study, we demonstrated that telmisartan but not valsartan suppressed TNF-α–induced IL-6 expression through a PPARγ-dependent manner. Inhibition of NF-κB and C/EBPβ DNA binding activity by telmisartan may be responsible for attenuation of TNF-α–induced IL-6 expression. This is the first study demonstrating that telmisartan modulates cytokine production induced by non–Ang II stimulus. The in vivo and ex vivo results were consistent with those obtained from the in vitro study. The in vivo study showed that telmisartan had an anti-inflammatory effect in mice, and the ex vivo study indicated that IL-6 was produced from blood vessel in response to TNF-α stimulation, and telmisartan attenuated the induction.

On activation by ligands, PPARγ regulates expression of several genes involved in lipid and carbohydrate metabolism and inflammatory responses.[21] PPARγ regulates gene expression through 2 different transcriptional regulatory mechanisms: transactivation and transrepression. Transactivation depends on PPARγ response element. On activation, PPARγ forms a heterodimer with retinoid X receptor and binds to PPARγ response element in the promoter region of the target genes.[22] In contrast, transrepression involves an interference with other transcription factors such as NF-κB and activator protein 1.[22] Although telmisartan was reported to be a partial agonist of PPARγ, it has not been determined whether telmisartan regulates gene expression through transrepression mechanism. Our data suggest that telmisartan may have a transrepression effect on gene expression in addition to AT1R blockade.

The mechanism of transrepression by PPARγ activators is less well known. A recent study showed that PPARγ activation by TZD induced sumoylation of PPAR, resulting in retention of nuclear receptor corepressor/histone deacetylase complex to the promoter and suppression of gene transcription.[12] Troglitazone, another TZD, inhibited TNF-α–induced and NF-κB–dependent gene transcription without affecting NF-κB nuclear translocation or DNA binding in adipocytes,[23] which may support the above-mentioned model. However, a previous study showed that TZDs inhibited IL-1β–activated NF-κB and C/EBPβ DNA binding to the IL-6 gene promoter.[24] It was also reported that troglitazone inhibited TNF-α–induced IL-6 expression in multiple myeloma cells by inhibiting NF-κB and C/EBPβ DNA binding.[25] In this study, activated PPARγ competed for PPARγ coactivator-1, a transcription coactivator, with NF-κB, resulting in attenua-

Table. Heart Rate and Blood Pressure of Ang II– and TNF-α–Treated Mice

Variable	Control	Tel	Ang II	Tel+Ang II	TNF-α	Tel+TNF-α
HR (bpm)	576±24	598±21	599±18	608±27	611±47	586±22
BP (mm Hg)	95.3±1.3	94.0±2.8	109.6±4.7*	102.2±1.8†	97.3±0.9	95.5±1.4

HR indicates heart rate; BP, blood pressure.
*$P<0.05$ vs control; †$P<0.05$ vs Ang II; n=5.

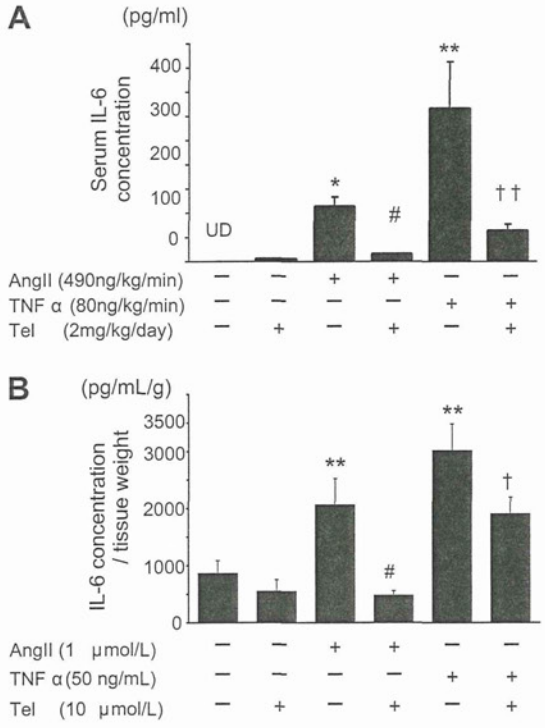

Figure 6. Telmisartan attenuated IL-6 production in vivo and ex vivo. A, Serum concentration of IL-6 was measured in mice injected with Ang II (490 ng/kg per minute) or TNF-α (80 ng/kg per minute) in the presence or absence of telmisartan (Tel; 2 mg/kg per day) administration for 1 week (No. of independent experiments was 5). *P<0.05; **P<0.01 vs control (no treatment); #P<0.05 vs Ang II; ††P<0.01 vs TNF-α. UD indicates undetectable. B, An aortic segment was stimulated ex vivo with Ang II (1 μmol/L) or TNF-α (50 ng/mL) in the presence or absence of Tel (10 μmol/L) in DMEM supplemented with 0.1% BSA for 48 hours. The concentration of IL-6 in the supernatant was measured and normalized with wet weight of the aortic segment (No. of independent experiment was 4 in duplicate). **P<0.01 vs control; #P<0.05 vs Ang II; †P<0.05 vs TNF-α.

tion of TNF-α–induced NF-κB DNA binding. In contrast, activated PPARγ physically interacted with C/EBPβ, suggesting that this protein–protein interaction attenuates the DNA binding of C/EBPβ. Although the precise mechanisms are not clear at this point, it may be possible that telmisartan inhibits NF-κB and C/EBPβ DNA binding activity through the same mechanism.

Inflammation plays a crucial role in the initiation and progression of atherosclerosis.[26] IL-6 enhanced VSMC growth induced by platelet-derived growth factor.[27] IL-6 also increased both monocyte chemoattractant protein-1 production and DNA synthesis of VSMCs, which may coordinate inflammatory and proliferative responses.[28] IL-6 is also a useful biomarker predicting future cardiovascular events.[29] TNF-α also enhances vascular inflammation. Blockade of TNF-α activity by soluble TNF-α receptor suppressed coronary artery neointimal formation after cardiac transplantation in rabbits.[30] Therefore, telmisartan inhibition of TNF-α–induced IL-6 expression, which was not observed by valsartan, may attenuate vascular inflammation.

A recent report showed that C/EBPβ was involved in IL-17–induced C-reactive protein expression in VSMCs.[31] Another report showed that C/EBPβ regulated monocyte chemoattractant protein-1 expression in the aorta of hyperinsulinemic rats.[32] These studies suggest that C/EBPβ is also involved in vascular inflammation. Because NF-κB is well known to regulate gene expression of various inflammatory molecules,[33] telmisartan inhibition of NF-κB and C/EBPβ may contribute to attenuation of a broad range of inflammatory responses of blood vessel. However, it is not clear at this point whether telmisartan modulates gene expression induced by TNF-α other than IL-6 induction.

TZDs were constantly reported to inhibit atherogenesis in various models. Rosiglitazone inhibited development of atherosclerosis in LDL receptor–deficient mice.[11] Rosiglitazone was also shown to have additive effects on plaque regression in the combination treatment with simvastatin in an atherosclerotic rabbit model.[34] AT1R antagonists were also reported to suppress atherogenesis. Strawn et al demonstrated that losartan attenuated atherogenesis in monkeys with hypercholesterolemia.[35] Based on these studies and our results, telmisartan may be more protective against vascular lesion formation attributable to PPARγ activation and AT1R antagonism.

Perspective

In the present study, we showed that telmisartan inhibited Ang II– as well as TNF-α–induced IL-6 expression in VSMCs, rat aorta, and mice. Inhibition of TNF-α–induced IL-6 expression was mediated by PPARγ. And inhibition of NF-κB and C/EBPβ DNA binding by telmisartan may be responsible for suppression of TNF-α–induced IL-6 expression. The dual inhibition (Ang II– and TNF-α–induced IL-6 expression) of the inflammatory cytokine production by telmisartan may be beneficial for treatment of not only hypertension but also atherosclerotic cardiovascular diseases. However, large clinical trials are needed to determine whether these unique properties of telmisartan cause better clinical outcome in cardiovascular disease prevention.

Sources of Funding

This study was supported in part by grants-in-aid for scientific research from the Ministry of Education, Culture, Sports, Science and Technology of Japan (19590867; T.I.). Q.T. was supported by the Japan–China Sasakawa Medical Fellowship.

Disclosures

None.

References

1. de Gasparo M, Catt KJ, Inagami T, Wright JW, Unger T. International union of pharmacology. XXIII. The angiotensin II receptors. *Pharmacol Rev*. 2000;52:415–472.
2. Ferrario CM. Role of angiotensin II in cardiovascular disease therapeutic implications of more than a century of research. *J Renin Angiotensin Aldosterone Syst*. 2006;7:3–14.
3. McMurray JJ, Ostergren J, Swedberg K, Granger CB, Held P, Michelson EL, Olofsson B, Yusuf S, Pfeffer MA. Effects of candesartan in patients with chronic heart failure and reduced left-ventricular systolic function taking angiotensin-converting-enzyme inhibitors: the CHARM-Added trial. *Lancet*. 2003;362:767–771.
4. Barnett AH, Bain SC, Bouter P, Karlberg B, Madsbad S, Jervell J, Mustonen J. Angiotensin-receptor blockade versus converting-enzyme inhibition in type 2 diabetes and nephropathy. *N Engl J Med*. 2004;351:1952–1961.